J. Chem. Sci. (2018) 130:124
https://doi.org/10.1007/s12039-018-1525-1

REGULAR ARTICLE

Relative reactivity of N,N-donor ligands in substitution reactions of *cis*-diaqua(2-aminomethylpiperidine)platinum(II): a detailed kinetic and mechanistic study

DEBABRATA NANDI[a], SUMON RAY[a], PARNAJYOTI KARMAKAR[b], ANIMESH CHATTOPADHYAY[a], ANWESHA DEY[a], ROSHNI SARKAR(SAIN)[a] and ALAK K GHOSH[a,*]

[a]Department of Chemistry, The University of Burdwan, Burdwan, West Bengal 713 104, India
[b]Government General Degree College at Kalna-1, Muragacha, Medgachi, Burdwan, West Bengal 713 405, India
E-mail: alakghosh2002@yahoo.co.in

MS received 21 February 2018; revised 9 June 2018; accepted 22 June 2018; published online 23 August 2018

Abstract. The reactivity of *cis*-$[Pt(pipen)(H_2O)_2]^{2+}$ (pipen = 2-aminomethylpiperidine) was investigated by studying the interaction with some didentate N,N-donor ligands, namely, dimethylglyoxime (L_1H), 1,2-cyclohexanedionedioxime (L_2H) and α-furildioxime (L_3H) in an aqueous medium. All the above substitution reactions have been monitored spectrophotometrically at 320, 308 and 290 nm, respectively, where the spectral difference between the reactants and the products are appreciable. The kinetic study has been substantiated by product isolation, UV, IR and ESI-MS spectroscopic analysis. The rate parameters have been evaluated under different reaction conditions. The reactions were found to occur in two consecutive steps. The mechanism of the substitution reactions appears associative in nature as supported by the large and negative values of $\Delta S^{\neq}$.

Keywords. Kinetics; platinum(II); 2-aminomethylpiperidine; vicinal dioximes.

1. Introduction

It is well-known that platinum complexes such as cisplatin, carboplatin and oxaliplatin are extensively used for the treatment of different types of cancer.[1] Negative side effects during treatment (such as vomiting, resistance, ototoxicity, neurotoxicity, cardiotoxicity, *etc*.) encouraged researchers to design new classes of platinum complexes with improved anti-tumour properties. The third generation anti-tumour complexes, such as orally active Pt(IV) complexes, sterically hindered Pt(II) complexes, polynuclear Pt(II) complexes and sulfur-containing platinum complexes, are now tested in pre-clinical trials.[2,3]

Although the precise mechanism underlying the anti-tumour action of platinum drugs is not fully understood, the activity has been accounted for in terms of the interaction between the metal complex and DNA, primarily by forming bifunctional adducts.[1] DNA is the main target of these drugs in tumour cells.[4] However, there are many other biomolecules that can also potentially react with Pt complexes, such as small molecules, proteins and enzymes.[5] Therefore, the modes of action of metal-based antitumor drugs require the study of their interactions with a range of possible biological targets including amino acids, hormones, peptides and proteins. It is well-known that once anti-tumour complexes are in the bloodstream they remain intact due to the relatively high concentration of chloride ions ($\sim 10^{-1}$ mol dm^{-3}). After entering into the cell, *via* either passive diffusion or active uptake, the complexes undergo aquation by which a chloride ligand is displaced by a molecule of water due to a much lower chloride ion concentration (3–20 mM) inside the cell. These hydrolyzed species bind to DNA in competition with sulfur-containing molecules that also have a high affinity for platinum.[6]

Here, the title complex is water soluble and has significant cytotoxic activity against cisplatin-resistant

*For correspondence

Electronic supplementary material: The online version of this article (https://doi.org/10.1007/s12039-018-1525-1) contains supplementary material, which is available to authorized users.

ovarian cancer cells.[7] Heterocyclic and chelating diamines both give compounds with noticeable activity; moreover, these carrier amine ligands appear to modulate the anticancer properties of this class of drugs.[8,9] The presence of an NH group in the 2-aminomethylpiperidine carrier ligand has led to the hypothesis that H-bonding interactions with a 50-terminal phosphate group and exocyclic O–6 guanine moiety within the platinated DNA influences its structure and activity.[10–12]

On the other hand, vicinal dioximes are important complexing ligands that have received considerable attention in biology and chemistry. They have also received attention due to their application in technology, imaging agents, analytical chemistry, optical, conductive, mesogene and redox properties. The ability of oxime-containing ligands to stabilize particular metal ion redox states is vitally important in their role in bioinorganic systems. Some vicinal dioximes also show antimicrobial properties.[13–18]

In this paper, we report the interaction of three vicinal dioximes with $[Pt(pipen)(H_2O)_2]^{2+}$ in aqueous medium and the possible mode of binding is also discussed.

2. Experimental

2.1 *Materials*

K_2PtCl_4 (98%, Sigma-Aldrich, USA), 2-aminomethylpiperidine (97%, Sigma-Aldrich, USA), 2,2′-Furildioxime (97%, Alfa Aesar, USA), 1,2-Cyclohexanedionedioxime (96%, Sigma-Aldrich, USA) and Dimethylglyoxime (99%, SRL, India) were purchased to carry the above kinetics. All other reagents used in this research were obtained from commercial sources and used without purification. A solution of the above-mentioned complex and other reagents except ligand used for this work were prepared freshly in double-distilled water before use. Kinetic studies were performed in 10% ethanol–water (v/v) mixture.

2.2 *Physical measurements*

The pH measurements were carried out with the help of a Sartorius Digital pH meter (model PB11) with an accuracy of ±0.01 units. Infrared (IR) spectroscopy on KBr pellets was performed on a Shimadzu FT-IR model IR Prestige 21 infrared spectrophotometer from 4,000 to 400 cm^{-1}. ESI-MS was recorded using a micromass Q-ToF micro™ mass spectrometer in positive ion mode. Electronic spectra and kinetic measurements were monitored on a Shimadzu spectrophotometer (UV-2450) equipped with a Shimadzu TCC 240A cell temperature controller (accuracy ±0.1 °C).

2.3 *Procedure and characterization*

The complex $[Pt(pipen)(H_2O)_2](ClO_4)_2$ termed as complex **1**, was prepared according to the literature.[19] The pH of the solution was so maintained (pH = 4.0) that >90% of the perchlorate salt was obtained as diaqua species. The reaction products of complex **1** with the above three vicinal dioximes (LH) were prepared by mixing the reactants in different ratios namely 1:5, 1:10, 1:20 and 1:30 and equilibrating the mixture at (30 ± 0.1) °C for 48 h. The absorption spectra of all these mixtures for each ligand exhibit the same λ_{max} with nearly identical intensities. The difference in spectra between the product complexes and the substrate complex is shown in Figure 1.

The composition in the solution was determined by Job's method of continuous variation. The metal: ligand ratio was found to be 1:1 (Figure 2). This fashion is also observed for the other two ligands.

As indicated from Job's method, complex **1** and the ligands were mixed in 1:1 molar ratio in a reaction vessel and heated at 60 °C for 72 h, then products were transferred in a glass beaker and slowly evaporated at room temperature and finally in a desiccator. The IR and ESI-MS measurements have been used for the characterization of the above products.

The IR spectra of the product, complex **1** with that of L_2H (in KBr disk) showed (Figure S1, Supplementary Information) strong characteristic bands at 3436 and 526 cm^{-1}, respectively. The strong band at 3436 cm^{-1} indicates that the product is hydrated or contained free -OH group. The stretching frequency at 526 cm^{-1} is assigned to υ(Pt–N) bond in the product.[20] The absence of a strong band of the Pt–O bond at 627 cm^{-1},[21] present in starting complex **1**, suggests the absence of Pt–O bond in the product complex. So the IR spectra strongly suggest that the final product is an (N,N) coordinated chelate and the 1,2-cyclohexanedionedioxime behaves as a bidentate ligand in the experimental pH. A typical ESI mass spectrum of the resulting product with ligand L_2H is shown in Figure 3.

It is clear from this spectrum that the ions at m/z ~ 450.84 are the protonated species of the product in the solution mixture and this is attributed to [Pt(II) + pipen + 1, 2-cyclohexanedionedioxime anion + H^+].

3. Results and Discussion

3.1 *Kinetic studies*

The kinetic measurements of these systems were done according to our previous work.[22] In this work the nature of the two typical plots ($\ln(A_\infty - A_t)$ vs time and $\ln\Delta$ vs time) are also the same as discussed in our previous work.[22] Origin software was used for computational analysis. Rate data, represented as an average of duplicate runs, were reproducible to within ±4%.

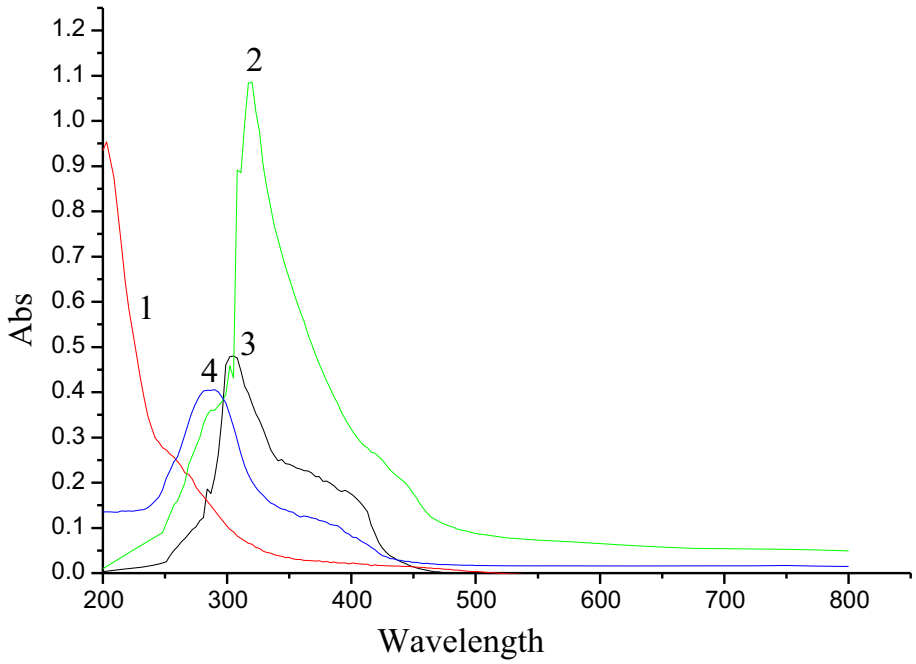

Figure 1. Spectra of the starting [complex**1**] = 1.85×10^{-4} M (1); complex**1** + [α-furil dioxime] = 3.7×10^{-3} M (2); complex**1**+[1, 2-cyclohexanedionedioxime] = 3.7×10^{-3} M (3); and the last one is complex **1** with that of [dimethylglyoxime] = 3.7×10^{-3} M (4), at pH = 4.0.

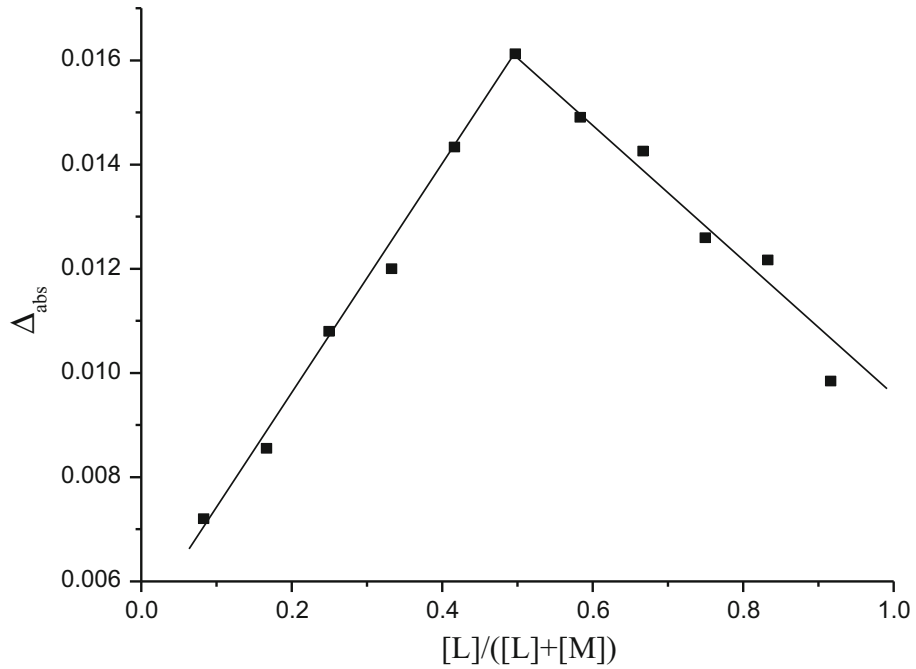

Figure 2. Job's plot for the reaction of complex **1** with L_2H at pH = 4.0 and ionic strength = 0.1 M $NaClO_4$.

The pKa values at 25 °C of the ligands L_1H, L_2H and L_3H are given in Table 1. From the pKa values of all the ligands we can say that at pH 4.0, all these three ligands remain in the neutral form.

On the other hand, the pK_1 and pK_2 values for *cis*-$[Pt(pipen)(H_2O)_2]^{2+}$ have been evaluated by Irving-Rossotti route[24] and found to be 6.45 and 7.96, respectively, at 25 °C. Hence, it can be assumed that at pH 4.0,

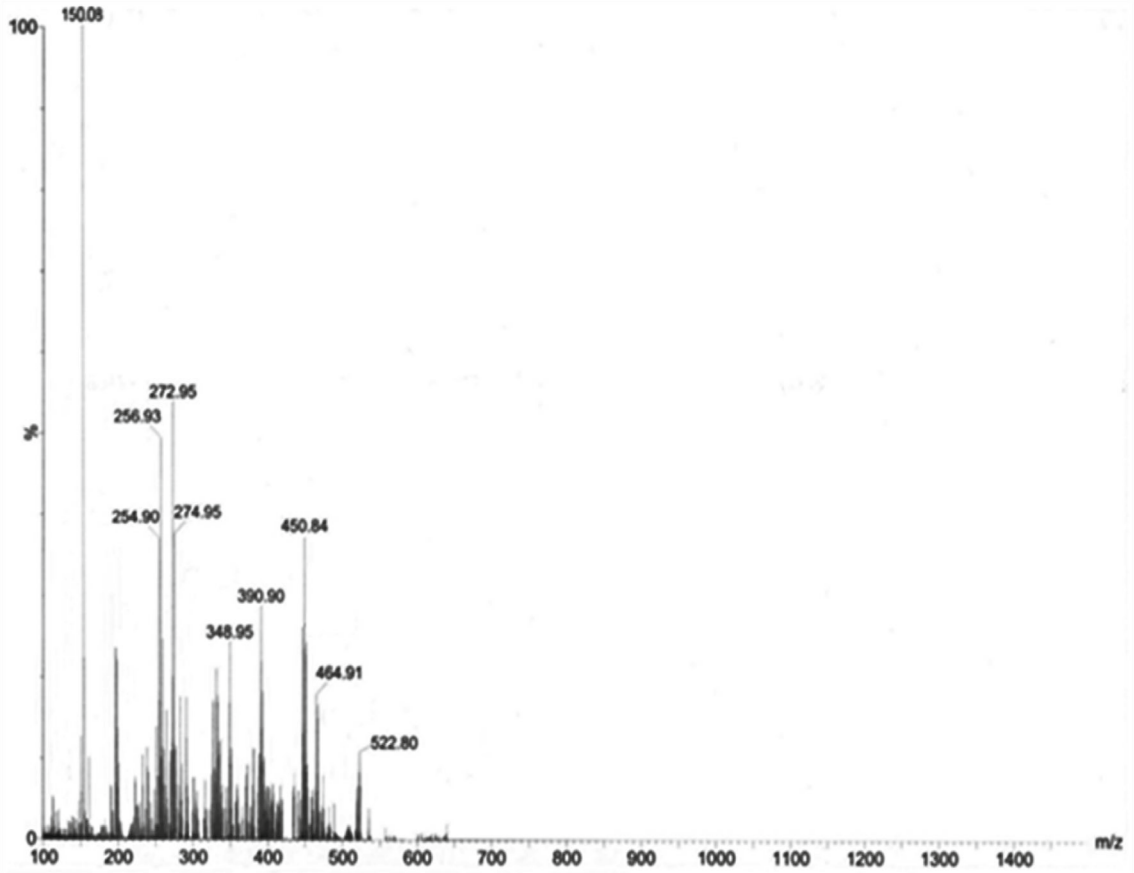

Figure 3. ESI-mass spectrum of the product complex **1** with that of L_2H.

Table 1. pKa values of three ligands named Dimethylglyoxime (L_1H), 1,2-Cyclohexane dionedioxime (L_2H) & α-Furildioxime (L_3H).

Ligands	Structures	Reference
Dimethylglyoxime (L_1H) $pK_1 = 10.66$	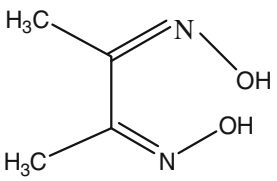	23
1,2-Cyclohexane dionedioxime (L_2H) $pK_1 = 12$	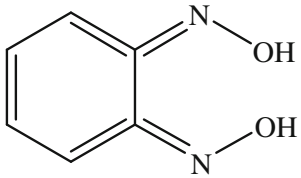	23
α-Furildioxime (L_3H) $pK_1 = 11.5$	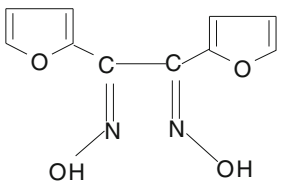	23

the reactant complex exists as diaqua ion. The reactions followed a two-step consecutive process; the first step is dependent on ligand concentration whereas the second is independent of ligand concentration. In the first step, one aqua ligand was replaced from complex **1** by ligands. The second is a slower step, where another water molecule is substituted. This is the ring closure step. The rate constant for such a process can be evaluated by assuming the following scheme:

$$A \xrightarrow{k_1} B \xrightarrow{k_2} C$$

Scheme 1.

where, A is the diaqua species (complex **1**), B is the single substituted intermediate, C is the final chelated product complex $[Pt(pipen)(L)]^+$. Formation of C from B is predominant after some time has elapsed.

3.1a *Calculation of k_1 for A → B step*: The rate constant for the first step, A → B was calculated from the absorbance data using the Origin 6.0 software, as discussed in our previous work.[22] The rate increases for all the three studied systems with increases in [ligand] before reaching a limiting value, (Figures 4, S2 and S3, Supplementary Information) which is probably due to the completion of the outer-sphere association complex formation through H-bonding.

The $k_{1(obs)}$ values for different concentrations of ligand at different temperatures are given in Table 2. Based on the experimental findings, the following scheme may be proposed:

$$[Pt(pipen)(H_2O)_2]^{2+} + LH \underset{}{\overset{K_E}{\rightleftharpoons}} [Pt(pipen)(H_2O)_2]^{2+}.....LH$$

Outer sphere association complex

$$[Pt(pipen)(H_2O)_2]^{2+}..... LH \xrightarrow[\text{anation}]{k_1} [Pt(pipen)(H_2O)(LH)]^{2+} + H_2O$$

$$[Pt(pipen)(H_2O)(LH)]^{2+} \xrightarrow[\text{chelation}]{k_2} [Pt(pipen)(L)]^{+} + H_3O^{+}$$

Scheme 2.

where, LH is the neutral form of the above ligands.

Based on Scheme 2, a rate expression can be derived as discussed in the earlier paper.[22] Depending upon the final equation as stated below.

$$1/k_{1(obs)} = 1/k_1 + 1/k_1 K_E[LH]$$

We have drawn a plot of $1/k_{1(obs)}$ versus $1/[LH]$. This plot should be linear with an intercept of $1/k_1$ and slope $1/k_1K_E$. This was found to be so, at all temperatures studied (Figure 5, Figures S4 and S5, Supplementary Information). The values of k_1 and K_E were obtained from the intercept and slope to intercept ratio respectively, and are included in Table 3.

3.1b *Calculation of k_2 for B → C step*: The B → C step is assigned to ring closure where another nitrogen

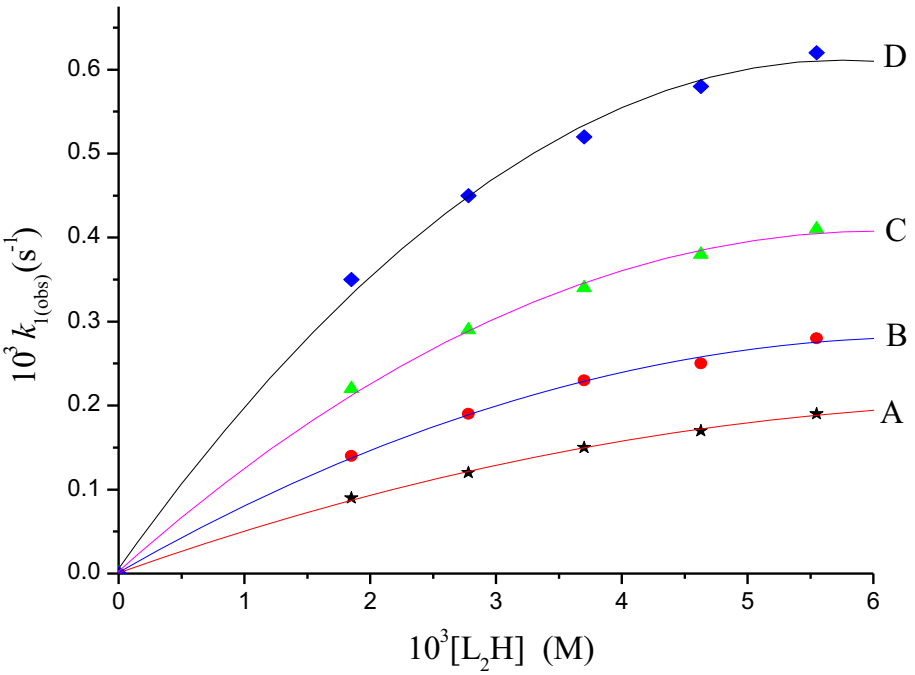

Figure 4. Plots of $k_{1(obs)}(s^{-1})$ versus $[L_2H]$ (M) at different temperatures. A = 30, B = 35, C = 40 and D = 45 °C.

Table 2. $10^3 \times k_{1(obs)}$ (s^{-1}) values for different ligand concentrations at different temperatures. [complex**1**] = 1.85×10^{-4} M, pH = 4.0, ionic strength = 0.1 M $NaClO_4$.

Ligands	Temp. (±0.1 °C)	10^3 [ligand] (M)				
		1.85	2.78	3.70	4.63	5.55
L_1H	30	0.30 ± 0.01	0.41 ± 0.02	0.50 ± 0.03	0.58 ± 0.04	0.65 ± 0.01
	35	0.41 ± 0.03	0.55 ± 0.01	0.66 ± 0.02	0.77 ± 0.03	0.83 ± 0.02
	40	0.60 ± 0.02	0.80 ± 0.03	0.95 ± 0.01	1.08 ± 0.02	1.19 ± 0.02
	45	0.89 ± 0.04	1.17 ± 0.01	1.38 ± 0.04	1.56 ± 0.01	1.70 ± 0.03
L_2H	30	0.22 ± 0.01	0.29 ± 0.02	0.38 ± 0.03	0.42 ± 0.02	0.48 ± 0.01
	35	0.32 ± 0.03	0.43 ± 0.01	0.52 ± 0.01	0.58 ± 0.03	0.65 ± 0.02
	40	0.41 ± 0.01	0.54 ± 0.02	0.67 ± 0.01	0.70 ± 0.01	0.81 ± 0.03
	45	0.49 ± 0.04	0.66 ± 0.03	0.80 ± 0.02	0.89 ± 0.02	0.97 ± 0.01
L_3H	30	0.19 ± 0.02	0.27 ± 0.03	0.34 ± 0.02	0.38 ± 0.03	0.43 ± 0.01
	35	0.28 ± 0.01	0.37 ± 0.01	0.46 ± 0.03	0.52 ± 0.01	0.57 ± 0.04
	40	0.38 ± 0.03	0.49 ± 0.04	0.60 ± 0.04	0.67 ± 0.02	0.73 ± 0.03
	45	0.45 ± 0.04	0.56 ± 0.02	0.73 ± 0.03	0.81 ± 0.04	0.88 ± 0.01

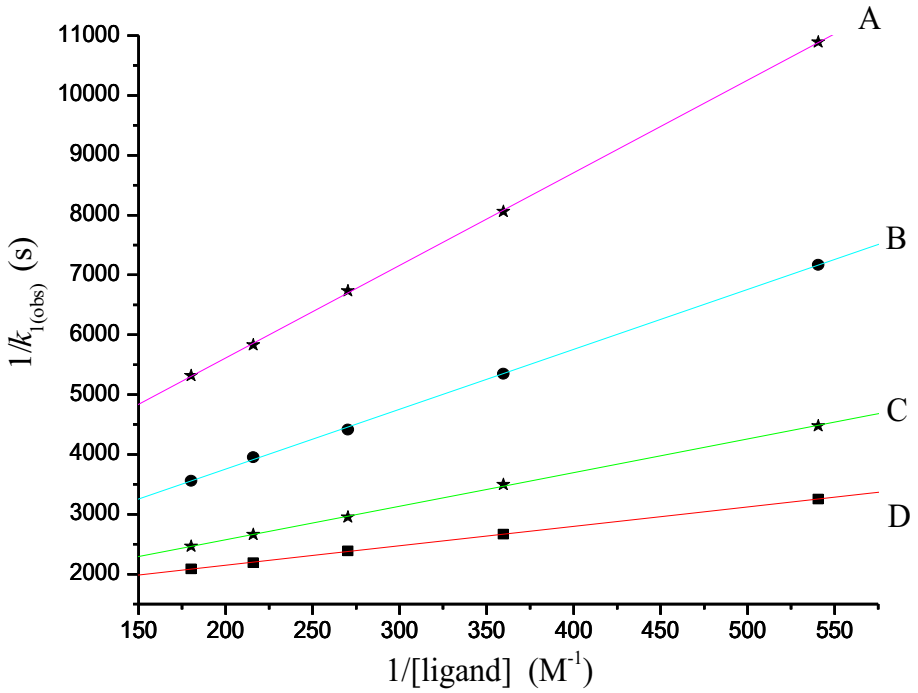

Figure 5. Plots of $1/k_{1(obs)}$ (s) versus $1/[L_2H]$ (M^{-1}) at different temperatures A = 30, B = 35, C = 40 and D = 45 °C for complex **1**.

atom of those ligands bind the metal center. This chelation step is independent of ligand concentration. At each temperature, the k_2 values were calculated from the limiting linear portion (when t is large) of the ln ($A_\alpha - A_t$) versus t curves and are collected in Table 3.

3.2 *Effects of pH on the reaction rate*

The reaction was studied at four different pH values. At a fixed 1.85×10^{-4} M [complex **1**], 3.7×10^{-3} M [ligand], and 0.1 M $NaClO_4$ ionic strength, the $10^3 k_{1(obs)}$ values were 0.11, 0.25, 0.38, 0.51, 0.66 and $10^5 k_2$ values were 0.48, 0.79, 1.23, 1.75, 1.99, respectively, for complex **1** with that of L_2H at pH 3.0, 3.5, 4.0, 4.5 and 5.0, respectively, at 30 °C. The change in rate may be explained based on two acid dissociation equilibria of the ligand and for the complex. At low pH (~3.0) there may be the protonated species of vicinal dioximes exists and with an increase in pH, they are transformed into the neutral species and the reaction rate increases. Complexes might not be affected in the studied pH range, or

Table 3. The k_1, k_2, K_E values for the substitution reaction between different ligands with complex **1**.

Ligands	Temp. (°C)	$10^3 k_1 (s^{-1})$	K_E (M^{-1})	$10^5 k_2 (s^{-1})$
L_1H	30	1.54 ± 0.04	131 ± 0.01	1.45 ± 0.01
	35	1.75 ± 0.03	165 ± 0.02	1.92 ± 0.03
	40	2.32 ± 0.01	188 ± 0.04	2.63 ± 0.02
	45	3.11 ± 0.05	216 ± 0.01	3.25 ± 0.01
L_2H	30	0.40 ± 0.05	162 ± 0.05	1.23 ± 0.04
	35	0.57 ± 0.04	175 ± 0.03	1.71 ± 0.03
	40	0.69 ± 0.02	259 ± 0.01	2.27 ± 0.02
	45	1.01 ± 0.01	293 ± 0.04	2.89 ± 0.01
L_3H	30	0.22 ± 0.04	177 ± 0.02	0.98 ± 0.04
	35	0.30 ± 0.01	248 ± 0.05	1.41 ± 0.05
	40	0.41 ± 0.05	317 ± 0.01	1.92 ± 0.01
	45	0.62 ± 0.01	373 ± 0.04	2.51 ± 0.02

we can't explain the phenomenon with the formation of hydroxoaqua species, because the highest pH value of study (i.e., 5.0) is far apart from the first pKa values of the complexes (i.e., 6.45 and 7.96, respectively). So the effects of pH on rate are therefore due to the change in reactive forms of the reacting ligands.

3.3 *Effect of substituents in the ligand structure*

If two methyl groups in L_1H are successively replaced by cyclohexane ring in L_2H and two furan rings in L_3H, the substituent effect shows that there is a gradual decrease of rate constant values from L_1H to L_3H through L_2H. For L_1H, L_2H and L_3H, the relative λ_{max} positions of LH-substituted products are found to be at 320, 308 and 290 nm, respectively (Figure 1). It is a clear evidence of weak donicity trend as a sharp lower energy shift of λ_{max} observed for complexes L_1H to L_3H through L_2H. The measurement of rate constant values depends on both electronic and steric factors. For an associative activation with an increase in the size of the incoming ligand, the activated state is crowded and as a result, a decrease in rate with increased crowding is observed. This also supports a ligand-assisted mechanism.

3.4 *Effects of temperature on the reaction rate*

Those reactions were monitored at four different temperatures for diverse ligand concentrations and the substitution rate constants for both A $\rightarrow$ B (k_1) and B $\rightarrow$ C (k_2) steps are arranged in Table 3. The activation parameters calculated from Eyring plots (Figure 6, and Figures S6 and S7, Supplementary Information) are tabulated in Table 4.

3.5 *Mechanism*

The interaction of dimethylglyoxime (L_1H), 1,2-cyclohexane dionedioxime (L_2H) and α-furil dioxime (L_3H) with the title platinum complex proceeds *via* two distinct consecutive steps ($k_1 \sim 10^{-3}$ s^{-1} and $k_2 \sim 10^{-5}$ s^{-1}). The first step proceeds *via* an associative interchange activation and the second step is the ring closure. At the outset of the first step outer sphere association complex, a cage-like structure is formed possibly stabilized through H-bonding, with an increase in ligand concentration as more ligands come to the vicinity of the reactant complex and form H-bonding interaction. Henceforth, due to greater ligand concentration, rate constants for the substitution process also increases but ultimately the H-bonded ligands around the complex form a cage-like structure and further H-bonding is not possible, which means that an equilibrium is reached. At equilibrium with an increase in ligand concentration, ligand molecules around the reactant complex remain same; hence, the rate constants remain unaltered and saturation is observed. The outer sphere association equilibrium constants, a measure of the extent of H-bonding for each path at different temperatures are evaluated (Table 3). A typical plot of $\ln K_E$ vs $1/T$ for complex**1** with L_3H is drawn in Figure 7. From the slope and intercept values, the thermodynamic parameters (ΔH^0 & ΔS^0) were also calculated (Table 5), which gives a negative ΔG^0 value at all temperatures studied, supporting the spontaneous formation of an outer sphere association complex in the first step.

From the temperature dependence of the k_1 and k_2 values the activation parameters were also calculated, $\Delta H_1^{\neq} = 35.6 \pm 4.8$kJ mol^{-1}, $\Delta S_1^{\neq} = -182 \pm 15$ J K^{-1} mol^{-1} (for L_1H), $\Delta H_1^{\neq} = 44.5 \pm 3.9$ kJ mol^{-1}, $\Delta S_1^{\neq} = -163 \pm 12$ J K^{-1} mol^{-1} (for L_2H) and $\Delta H_1^{\neq} =$

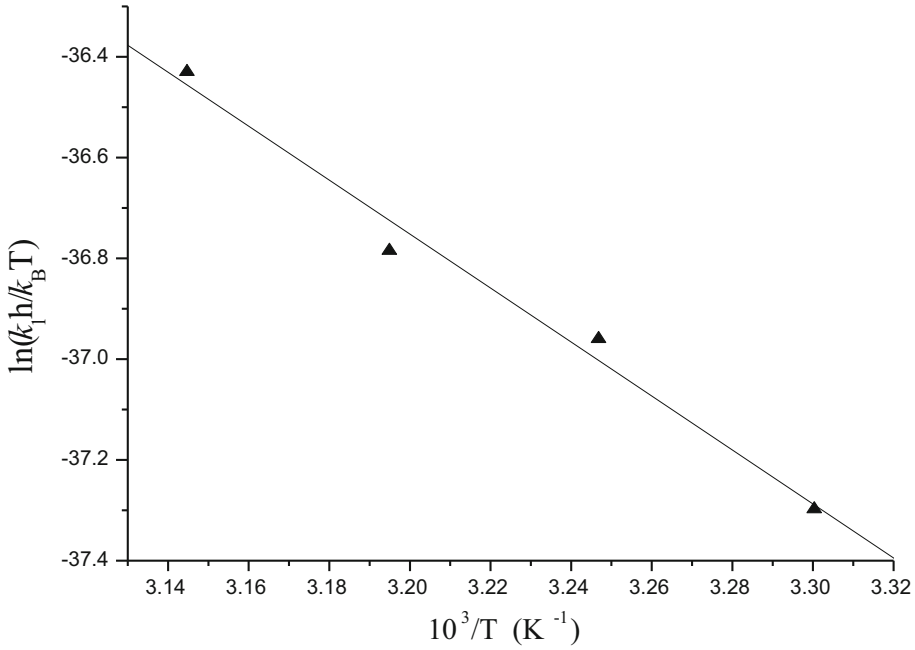

Figure 6. Eyring plot of $\ln(k_1 h/k_B T)$ versus 1/T for the step A → B (For complex **1** with L_2H).

Table 4. Activation parameters for the analogous systems by the above three vicinal dioximes in an aqueous medium at pH = 4.0.

Systems	$\Delta H_1^{\neq}$ (kJ mol^{-1})	$\Delta S_1^{\neq}$ (J K^{-1} mol^{-1})	$\Delta H_2^{\neq}$ (kJ mol^{-1})	$\Delta S_2^{\neq}$ (J K^{-1} mol^{-1})	Ref.
$[Pt(en)(H_2O)_2]^{2+}/L_1H$	20.9 ± 1.5	-164 ± 4	31.6 ± 2.3	-226 ± 7	[22]
$/L_2H$	27.4 ± 1.9	-214 ± 9	35.2 ± 3.4	-218 ± 11	
$/L_3H$	30.6 ± 1.7	-205 ± 5	38.4 ± 2.3	-209 ± 7	
$[Pt(pipen)(H_2O)_2]^{2+}/L_1H$	35.6 ± 4.8	-182 ± 15	41.3 ± 2.0	-201 ± 7	This work
$/L_2H$	44.5 ± 3.9	-163 ± 12	43.1 ± 1.8	-197 ± 6	
$/L_3H$	52.2 ± 3.4	-143 ± 11	47.6 ± 1.9	-184 ± 6	

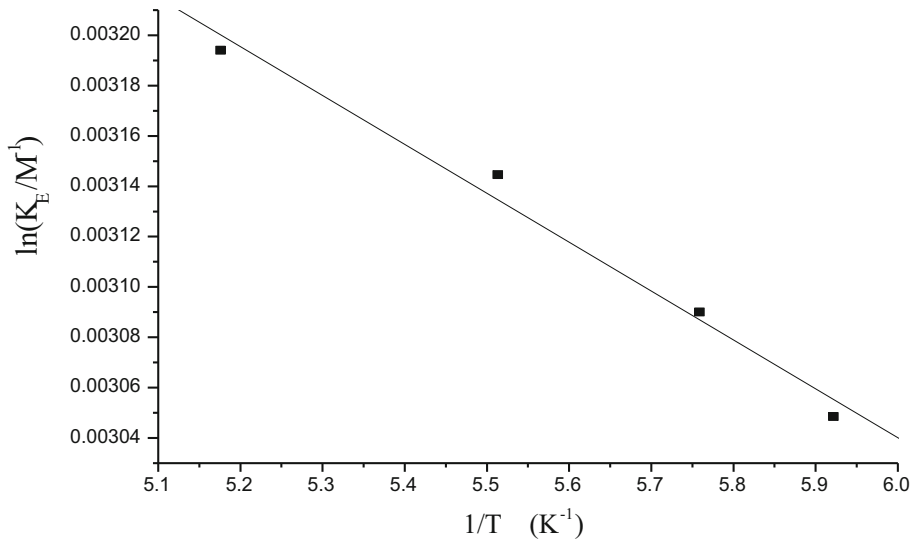

Figure 7. A typical plot of $\ln(K_E/M^{-1})$ vs $1/T$ (K^{-1}) (for complex **1** with L_3H).

52.2 ± 3.4 kJ mol^{-1}, $\Delta S_1^{\neq} = -143 \pm 11$ J K^{-1} mol^{-1} (for L_3H), respectively. There occurs the formation of the five-membered structure of the product by the coordination of two nitrogen atoms of LH with the Pt(II) center. Now one nitrogen atom first attacks one of the Pt(II) centre by the removal of one water molecule (k_1 path) and another nitrogen atom of the LH finishes the ring closing process (k_2 path) by the removal of a second water molecule. After the above rigorous analysis, we propose the following reaction mechanism (Figure 8):

Table 5. Thermodynamic parameters for the above system by the above three ligands in an aqueous medium, pH = 4.0.

Ligands	ΔH^0 (kJ mol^{-1})	ΔS^0 (J K^{-1} mol^{-1})
L_1H	2.46 ± 0.24	38.6 ± 1.2
L_2H	1.77 ± 0.31	35.5 ± 1.6
L_3H	1.62 ± 0.15	35.0 ± 0.8

4. Conclusions

From a comparison of the ligands used, it can be concluded that the variation in bulkiness and electronic

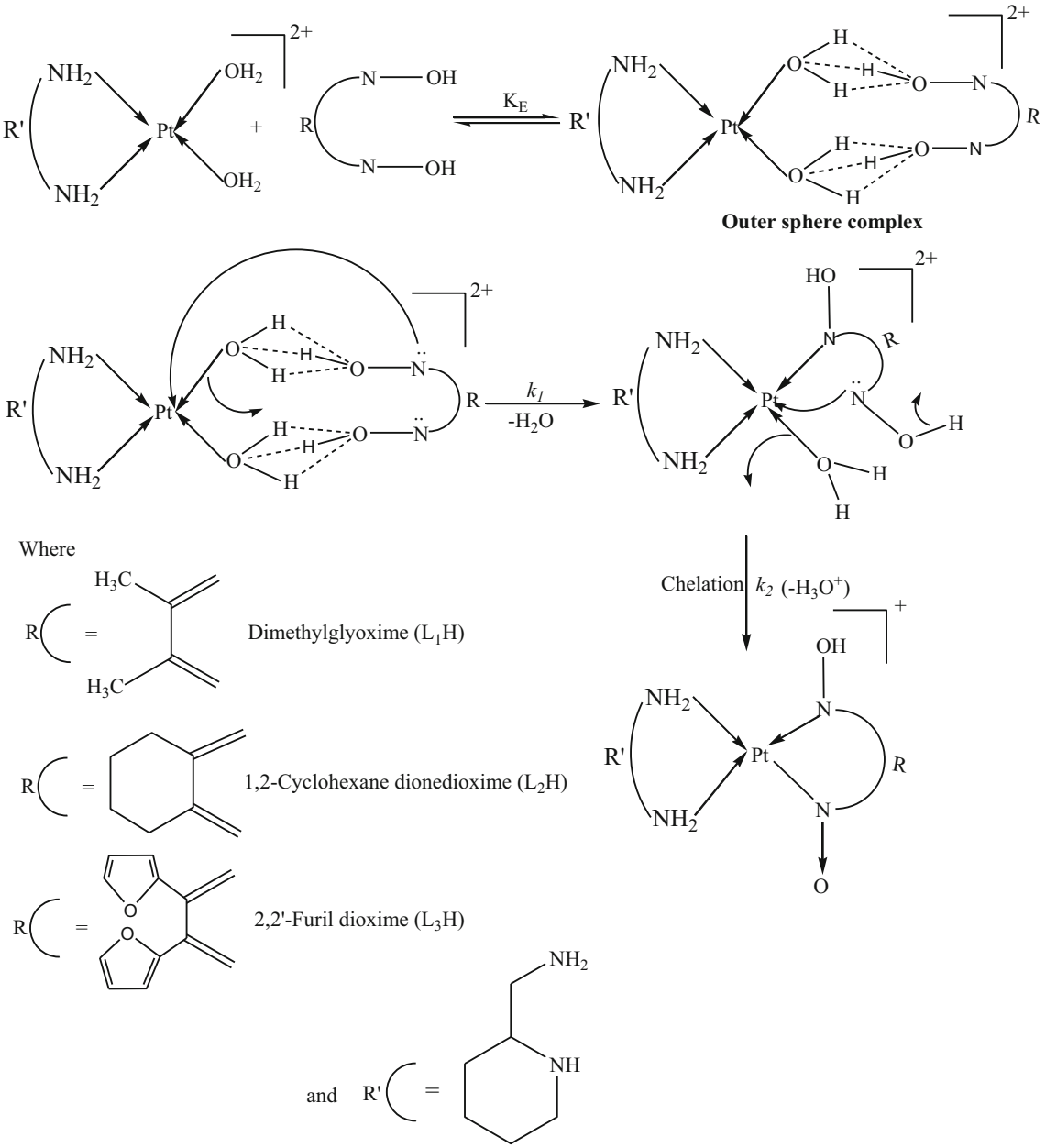

Figure 8. Plausible mechanism for the substitution of aqua ligands from $[Pt(pipen)(H_2O)_2]^{2+}$ by three vicinal dioximes.

effect of the entering vicinal-dioximes is reflected in their properties as nucleophiles. The differences in nucleophilicity of the ligands are obvious and their reactivity follows the order:

$$L_3H < L_2H < L_1H$$

The sensitivity of the reaction rate towards donor properties of the entering ligands are in line with that expected for an associative mode of activation. Due to the highest steric effect, the reactivity of the ligand (L_3H) was lowest which reflects in the rate constant values. Besides, the reactivity of the complexes follows the trend, as:

$$cis\text{-}[Pt(en)(H_2O)_2](ClO_4)_2 > cis\text{-}[Pt(pipen)(H_2O)_2](ClO_4)_2$$

The platinum(II) center in Pt(pipen) is less electrophilic due to the positive inductive effect (i.e., +I effect) of the piperidine ring compared to that of ethylenediamine. Higher the electrophilicity of the metal center, smaller is the activation enthalpy and hence the above order of reactivity has been observed. Further, *cis*-$[Pt(pipen)(H_2O)_2](ClO_4)_2$ complex is the sterically most crowded one, and the reactions are found to be slower than that of *cis*-$[Pt(en)(H_2O)_2](ClO_4)_2$.

Supplementary Information (SI)

For the characterization of the ligand substituted product complexes, figures such as IR spectra (Figure S1) and rate constant related graphs (Figures S2–S7) are given in the Supplementary Information, available at www.ias.ac.in/chemsci.

Acknowledgements

The authors are grateful to the Department of Chemistry, University of Burdwan, Purba Bardhaman, West Bengal, India for extending all types of co-operation and providing infrastructural facilities during this work.

References

1. (a) Wang D and Lippard S J 2005 Cellular processing of platinumanticancer drugs *Nat. Rev. Drug Discov.* **4** 307; (b) Zutphen S van and Reedijk J 2005 Targeting platinum anti-tumourdrugs: Overview of strategies employed to reduce systemic toxicity *Coord. Chem. Rev.* **24** 2845; (c) Zorbas H and Keppler B K 2005 Cisplatin damage: are DNA repair proteins saviors or traitorsto the cell? *Chem. Bio. Chem.* **6** 1157
2. Esposito B P and Najjar R 2002 Interactions of antitumoral platinum-group metallodrugs with albumin *Coord. Chem. Rev.* **232** 137
3. Ray S, Karmakar P, Chattopadhyay A, Nandi D, Ukil S, (Sain) R Sarkar and Ghosh A K 2016 Substitution reactions of [Pd(bipy)(malonate)] explored with a different set of ligands: Kinetic and mechanistic interpretation in aqueous medium and at pH 7.4 *J. Chem. Sci.* **128** 1327
4. Ho Y P, Au-Yeung S C F and To K K W 2003 Platinum-based anticancer agents: Innovative design strategies and biological perspectives *Med. Res. Rev.* **23** 633
5. Hacker M P and Douple E B 1984 In *Platinum Coordination Compounds in Cancer Chemotherapy* I H Krakoff (Ed.) (Boston: Martinus Nijhoff Pub)
6. Pil P and Lippard S J 1997 In *Encyclopedia of Cancer* J R Bertino (Ed.) (San Diego: Academic Press) p. 392
7. Abu-Surrah A S and Kettunen M 2006 Platinum group antitumor chemistry: design and development of new anticancer drugs complementary to cisplatin *Curr. Med. Chem.* **13** 1337
8. Wong H C, Coogan R, Intini F P, Natile G and Marzilli L G 1999 New Steric Hindrance Approach Employing the Hybrid Ligand 2-Aminomethylpiperidine for Diminishing Dynamic Motion Problems of Platinum Anticancer Drug Adducts Containing Guanine Derivatives *Inorg. Chem.* **38** 777
9. Goto M, Yamamoto Y, Sumimoto M, Tsuruda N and Kurosaki H 2003 Conformation of 2-Aminomethylpyrrolidine and 2-Aminomethylpiperidine in Ternary Platinum(II) Complexes: Regulation of Conformation of the Diamine by the Coexisting Ligand *Chem. Pharm. Bull.* **51** 1157
10. Sherman S E, Gibson D, Wang A H J and Lippard S J 1988 Crystal and molecular structure of cis-$[Pt(NH_3)_2\{d(pGpG)\}]$, the principal adduct formed by cis-diamminedichloroplatinum(II) with DNA *J. Am. Chem. Soc.* **110** 7368
11. Xu Y, Natile G, Intini F P and Marzilli L G 1990 Stereochemically controlled ligands influence atropisomerization of platinum(II) nucleotide complexes. Evidence for head-to-head and stable.LAMBDA. head-to-tail atropisomers *J. Am. Chem. Soc.* **112** 8177
12. Guo Z, Sadler P J and Zang E 1997 Recognition of platinum(ii) aminecomplexes by nucleotides: roleofphosphate and carbonyl groupsin($[^{15}N_3]$diethylenetriamine)-(guanosine5′-monophosphate)platinum(ii) *Chem. Commun.* 27
13. Tas E, Cukurovali A and Kaya M 1998 Synthesis of a new glyoxime derivative, characterization and investigation of its complexes with Ni (II), Co (II), Cu (II) and UO_2 (VI) metals *J. Coord. Chem.* **44** 109
14. Chakravorty A 1974 Structural chemistry of transition metal complexes of oximes *Coord. Chem. Rev.* **13** 1
15. Kandaz M, Coruhlu S Z, Yilmaz I and Ozkaya A R 2002 A novel (*E*, *E*)-dioxime and its mono-, di- and trinuclear complexes bearing tetradentate octyl sulfanyl phenylamino substituents. Synthesis, characterization and electrochemical properties of its transition metal complexes *Trans. Met. Chem.* **27** 877
16. Kurtoglu M, Dagdelen M M and Toroglu S 2006 Synthesis and Biological Activity of Novel (*E*, *E*)-*vic*-dioximes *Trans. Met. Chem.* **31** 382
17. Canpolat E, Kaya M and Gur S 2004 Synthesis, characterization of some Co (III) complexes with vic-dioxime

ligands and their antimicrobial properties *Turk J. Chem.* **28** 235
18. Musluoglu E and Ahsen V 1999 Synthesis and Characterization of 1,2-Bis(aziridin-*N*-yl)glyoxime and its Nickel(II), Palladium(II) and Cobalt(II) Complexes *J. Chem. Res. (S)* 142
19. Karmakar P 2014 The effect of σ-donation on the interactions of cis-diaqua (2-aminomethylpiperidine) platinum (II) complex with biomolecules in aqueous medium: synthesis, kinetic *Trans. Met. Chem.* **39** 727
20. Arpalahti J and Lehikoinen P 1989 Competition of various cis-Pt(II) diamines for the N1 and N7 sites of adenosine and 9-(β-D-ribofuranosyl)purine *Inorg. Chim. Acta* **159** 115
21. Behnke G T and Nakamoto K 1968 Infrared spectra and structure of acetylacetonatoplatinum(II) complexes. III. Infrared spectra of acetylacetonatoplatinum(II) complexes containing oxygen-bonded (chelated) and C-bonded acetylacetones *Inorg. Chem.* **7** 330
22. Nandi D, Chattopadhyay A, Ray S, Acharjee A, Sarkar(Sain) R, Laskar S and Ghosh A K 2016 Kinetic and mechanistic studies on thesubstitution of aqua ligands from diaquaethylenediamineplatinum(II)ion by vicinal dioximes *Monatsh. Chem.* **147** 1015 (and references therein)
23. Sillen L G and Martell A E 1964 In *Stability Constants of Metal-ion Complexes* J Bjerrum (Ed.) (Great Britain: Royal Society of Chemistry) Special publication no. 17
24. Irving H M and Rossotti (Mrs.) H S 1954 The calculation of formationcurves of metal complexes from pH titration curves in mixed solvents *J. Chem. Soc.* 2904